

Crack Blunting Effects on Dislocation Emission from Cracks

S. J. Zhou* and A. E. Carlsson

Department of Physics, Washington University, St. Louis, Missouri 63130

Robb Thomson

Materials Science and Engineering Laboratory, National Institute of Standards and Technology, Gaithersburg, Maryland 20899

(Received 15 November 1993)

A series of atomistic calculations is performed in order to establish criteria for dislocation emission from cracks in a model hexagonal lattice. We find that except for special orientations, additional tensile broken-bond effects must be added to existing theories based on shear effects, in order to correctly estimate the critical stress intensity K_e required for dislocation emission. From this, a new ductility criterion for materials is proposed which does not depend on the intrinsic surface energy, but contains only the unstable stacking fault parameter.

PACS numbers: 61.72.Lk, 61.43.Bn, 61.72.Yx, 62.20.Fe

A material is said to be intrinsically ductile (or brittle) if a sharp crack emits a dislocation at stress-intensity levels below that where crack cleavage occurs (or vice versa), because, except in special geometries, the emitted dislocation blunts the crack and renders it uncleavable. Other aspects of material microstructure also contribute to the ductile/brittle dichotomy, such as shielding by externally generated dislocations, weak cleavage surfaces at interfacial boundaries, etc. However, the intrinsic stability of the bonds at a crack tip against shear breakdown and dislocation formation is thought to be the underlying reason why certain broad classes of materials such as the fcc metals are generally ductile, and others such as ceramics are generally brittle [1].

There have been several attempts [1-4] to develop analytic, continuum-based estimates of the critical stress-intensity factor for emission, K_{Ie} . [One deals with the stress-intensity factor [5], defined by $\sigma(r) = K/\sqrt{2\pi r}$, rather than the stress σ itself, because the latter diverges near the crack tip.] There have also been several atomistic calculations [6-8]. The most successful continuum-based analysis has recently been performed by Rice [4], who found that for plane stress the critical stress-intensity factor for emission, K_{Ie} , is given by

$$K_e = \sqrt{2\gamma_{us}\mu(1+\nu)Y}, \quad (1)$$

where μ is the shear modulus, $\nu=0.25$ is Poisson's ratio, Y is a geometric factor given by the angle of dislocation emission, and γ_{us} is the "unstable stacking energy." The latter is defined as the maximum energy barrier encountered when two semi-infinite blocks of material are sheared relative to one other, and is thus a measure of the theoretical shear strength of the material. For simple lattices, the maximum energy barrier corresponds to a relative displacement of $b/2$ between the blocks, where b is the magnitude of the dislocation's Burgers vector. In Rice's analysis, this implies that the crack-tip dislocation is precisely half formed at the critical point of emergence.

In a systematic atomistic analysis [9], we have found that Eq. (1) is very accurate for a two-dimensional hex-

agonal model, using a "mode II" geometry in which an edge dislocation is emitted along the cleavage plane ahead of the crack. Here, we study emission in a more general geometry, and show that additional tensile effects can dominate the shear effects emphasized by Eq. (1) in that case. We use a lattice Green's-function methodology [10] for treating the boundary conditions, as in Ref. [9], and in this lattice, Poisson's ratio is always $\nu=0.25$.

Figure 1 shows a part of the nonlinear region in the cohesive zone, for our geometry, which allows both for crack propagation to the right and for dislocation emission along the "spur" at 60° to the crack plane. The loading forces are applied vertically, so that the crack is in pure "mode I" loading; under this form of loading, the 60° emission plane is the favored one according to elasticity theory [5]. K_{Ie} (K_I denotes a stress-intensity factor for mode I loading) is obtained by ramping up the force gradually; in frame (a) the dislocation is just about to appear, and in frame (b) it has been emitted and sits on the slip plane just out of range of the figure.

In order to evaluate the relative importance of key physical factors, we vary the attractive part of the force law, using a form which generalizes the universal binding energy relation (UBER) form [11]:

$$F^a = -kue^{-(u/l)^a}. \quad (2)$$

Here, u is the radial displacement between two atoms, relative to their equilibrium position, l is a length-scale parameter, and a varies the shape of the force law; the UBER form is obtained for $a=1$. For the repulsive part of the force law, we always use $a=1$ since we feel that the dominant chemical variations between materials lie in the attractive part of the force law. Because the brittle versus ductile behavior of the crack is independent of overall scaling factors in the potentials, we choose to normalize the potentials so that they have the same force constant k at the equilibrium separation. All of the forces are cut off slightly inside the second-neighbor distance, where $u=u_0=(\sqrt{3}-1)a$ and a is the nearest-neighbor spacing. In order to obtain force laws that van-

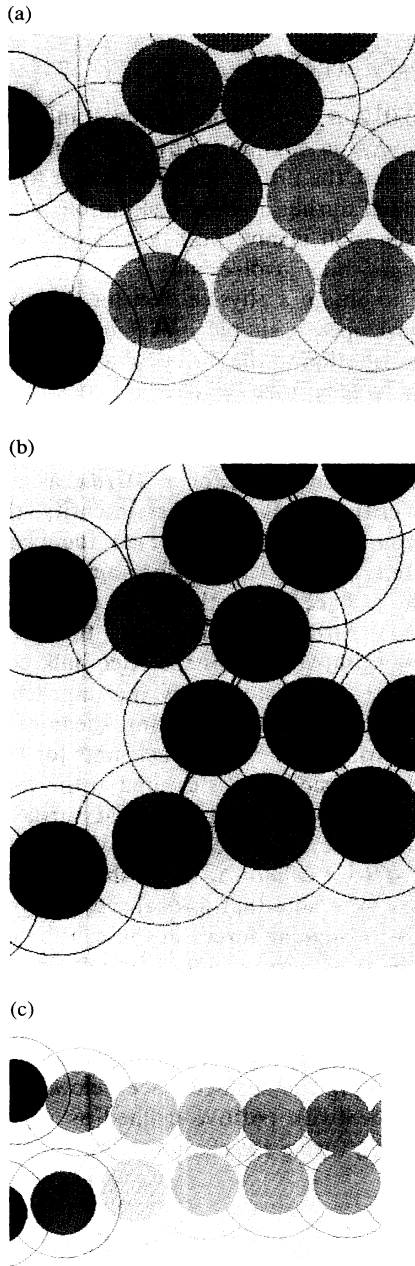


FIG. 1. Atomic positions near crack tip (a) immediately before emission in mode I; (b) immediately after emission in mode I; and (c) immediately before emission in mode II. Lighter shaded atoms are those which experience the greatest force contributions across the cohesive zone.

ish continuously at u_0 and preserve the force constant k , we have made a transformation on the form of F^a to obtain

$$\tilde{F}^a = -ku \frac{e^{-(u/l)^a} - e^{-(u_0/l)^a}}{1 - e^{-(u_0/l)^a}}. \tag{3}$$

For our purposes, the most important effects of changing

TABLE I. Data for ductile-to-brittle crossover. Superscripts "at" and "cont" denote estimates from atomistic calculations and continuum theory.

α	$K_{Ic}^{at}(k\sqrt{a})$	$K_{Ic}^{cont}(k\sqrt{a})$	$\Delta_c^{\parallel}(a)$	$\Delta_c^{\perp}(a)$
2.00	0.487	0.221	0.141	0.137
1.50	0.454	0.216	0.156	0.144
1.00	0.407	0.215	0.170	0.152
0.53	0.314	0.241	0.072	0.113

l are that with increasing l , the surface energy increases and the unstable stacking energy decreases.

Our results indicate that the mode I case is qualitatively different from the mode II case treated previously [9]. The most obvious indication of this is the atomic configuration immediately before emission, shown in detail in Fig. 1(a). Unlike the mode II case shown in Fig. 1(c), there is hardly any indication of a partly formed dislocation. We have obtained numerical values of the relative shear displacements on the slip plane, Δ_c^{\parallel} , by projecting the position of atom B on the line DC . As seen in Table I, Δ_c^{\parallel} is always less than the $b/2$ value obtained in the atomistic mode II results and predicted by the continuum theory. Thus the mode I emission geometry is very different from that of both the continuum results and the mode II atomistic results.

In general, it is not actually possible to evaluate K_{Ic} for a given force law, because if K_{Ic} differs significantly from the Griffith value [5] for crack propagation (under plane stress),

$$K_{Ic} = 2\sqrt{\gamma_s \mu(1+\nu)}, \tag{4}$$

then a stable crack cannot be obtained at a stress intensity of K_{Ic} —the crack will either close or run away to the end of the cohesive zone. However, in a given class of force laws, defined by a single value of α , one can find a value of l at which K_{Ic} is very near K_{Ic} , and a meaningful value of K_{Ic} can be obtained for this particular force law. Such results for K_{Ic} are given in Table I, and compared with the predictions of the continuum analysis. The atomistic results are roughly twice as high as those of the continuum theory for all values of α . Our estimates of K_{Ic} do not include the effects of the tensile stress on γ_{us} . As seen in Table I, the separation Δ_c^{\perp} between the atoms on either side of the slip plane is almost as large as the shear displacement, indicating strong tension-shear coupling. This will strongly reduce γ_{us} , increasing the discrepancy between the atomistic and continuum results.

In order to obtain a feel for the important parameters entering the brittle-ductile crossover in this case, we show in Fig. 2 a two-dimensional scatter plot of the force laws in which the force laws are plotted parametrized by their values of the surface energy γ_s and unstable stacking energy γ_{us} . We determined the critical values of γ_s and γ_{us} , where the model crossed over from brittle to ductile behavior, by assuming the material to be brittle if increas-

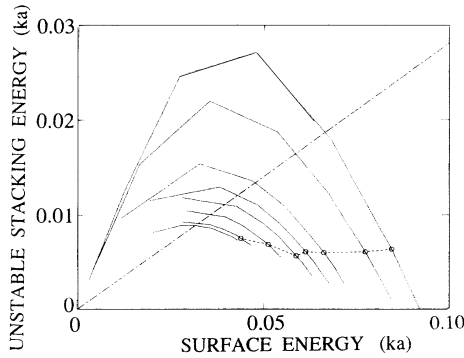


FIG. 2. Brittle vs ductile behavior as a function of γ_s and γ_{us} . Each line corresponds to a particular value of α [cf. Eqs. (2) and (3)]. From right to left, values of α are 2.0, 1.5, 1.0, 0.85, 0.75, 0.63, 0.53, and 0.5. Dashed line: brittle-ductile crossover. Points above this line have brittle behavior; points below it have ductile behavior. Dot-dashed line: prediction of Peierls model analysis of crossover (Ref. [4]).

ing the stress intensity over the Griffith value moves the crack tip past the dislocation spur, and ductile otherwise. The crossover points, where $K_{Ie} = K_{Ic}$, are given by the dot-dashed line in Fig. 2. In the continuum theory, the factor Y in Eq. (1) is $8/[(1 + \cos\theta) \sin^2\theta]$, where θ is the angle between the Burgers vector and the crack plane. Here, $\theta = 60^\circ$, so $Y = 64/9$. Therefore the brittle-to-ductile crossover in the continuum theory corresponds to the diagonal line $\gamma_{us}/\gamma_s = 9/32$ indicated in the figure. Because of constraints on the potentials, in our calculations we can obtain the crossover line only over a limited range of γ_s . In this range, the crossover is very different from that predicted by the continuum theory. It corresponds fairly closely to $\gamma_{us}/ka = 0.005$, or, using $b = a$ and the easily derived relationship $\mu = (\sqrt{3}/4)k$,

$$\gamma_{us}/\mu b = 0.012. \tag{5}$$

Thus the crossover is essentially independent of γ_s . (This does *not* imply that K_{Ie} is independent of γ_s , since the crossover is determined by the *ratio* of K_{Ie} and K_{Ic} , not by K_{Ie} itself.)

We believe that the source of the difference between these mode I results and the mode II case (both atomistic and continuum) is the extra energy involved in forming the free surface of the ledge which blunts the crack at its tip. Specifically, the ledge is represented by the missing bond at atom C in Fig. 1(b). This ledge energy is important because it is proportional to the free surface energy, γ_s , and γ_s is always considerably greater than γ_{us} , which dominates the emission criterion in mode II [cf. Eq. (1)].

Our introduction of the surface energy into the emission criterion above is consistent with the brittle-to-ductile crossover ($K_{Ie}/I_{Ic} = 1$) results seen in Fig. 2. The observed γ_{us} independence of the crossover [cf. Eq. (5)] requires that the dependence of K_{Ie} on γ_s be the same as that of K_{Ic} ; from Eqs. (4) and (5) we then arrive at the

form

$$K_{Ie} = 2\sqrt{\gamma_s\mu(1+\nu)}f(\gamma_{us}), \tag{6}$$

where $f(0.012\mu b) = 1$. The physical interpretation of this is that K_{Ie} is dominated by the surface energy required to blunt the crack. Further, since the ledge surface is created during a shear dislocation formation process, emission will involve both γ_{us} as well as γ_s , unlike pure cleavage which involves only γ_s .

In order to obtain a physical feel for the above results, we have developed a simple model based on a "surface excess" contribution to the dislocation misfit energy. The approach is to generalize the Rice [4] construction for the misfit energy Ω of an emerging dislocation distribution as a function of its position x , and then to find the maximum in the configurational force, or $-d\Omega/dx$, as a function of x . At the critical emission stress intensity, this force is precisely countered by that due to the elastic energy release rate. Because the dislocation formation takes place at the surface at the tip of the crack, we break Ω into bulk and surface contributions. thus $\Omega = \Omega^b + \Omega^s$, where $\Omega^b = \int_0^\infty \Phi[\Delta(x)]dx$ is the Rice bulk contribution, and $\Phi[\Delta(x)]$ is the misfit energy (per unit length) corresponding to the misfit $\Delta(x)$ during shear of an infinite body. The surface contribution accounts for the fact that in our case, the dislocation is created at the surface at the crack tip, and leaves a ledge on that surface. Because this additional energy is localized at the surface, we can write it as $\Omega^s(\Delta_s)$, where Δ_s is the shear displacement at the surface. (We note that a localized energy term such as Ω^s leads to singular forces in the continuum approximation if the ledge term is added into Φ as a simple surface tension [12]. However, at the atomic level, the forces creating the ledge surface are well behaved, and ramp up to the final surface energy value as the bonds stretch in making the surface. See below.) The configurational force (with positive defined as away from the surface) is then (using the chain rule for the surface part) given by

$$F = \frac{-d\Omega}{dx} = -\Phi(\Delta_s) - \beta_s(d\Omega^s/d\Delta_s), \tag{7}$$

where $\beta_s = d(\Delta_s)/dx$ is simply the strain in the dislocation distribution at the surface. The $d\Omega^s/d\Delta_s$ factor mainly results from the forces acting across the crack on the surface atoms. We find that the dominant contribution is just the slip plane component of the $A-B$ bond force, F_{A-B} , at the critical configuration shown in Fig. 1(a).

To obtain an emission criterion, we equate the maximum value of F with the elastic energy release rate, which is modified by the angle-dependent geometric factor $Y = 64/9$ as in Eq. (1). The result is that

$$\frac{1}{Y} \frac{K_{Ie}^2}{2\mu} = \Phi(\Delta_s) + \beta_s F_{A-B}. \tag{8}$$

To estimate how large the surface correction term might be, we use as an upper bound for β_s the maximum bulk dislocation value of β in the Peierls-Nabarro approach, which is $8\pi\gamma_{us}/(1+\nu)\mu b$ [9]. From our simulations, we find that the force F_{A-B} immediately before dislocation emission is roughly proportional to the surface energy, i.e., $F_{A-B} \approx 1.2\gamma_s$. Thus the maximal value of the surface term would be roughly $(25\gamma_{us}/\mu b)\gamma_s$. For all of the types of force laws for which we observed a brittle-to-ductile transition, this is considerably larger than the bulk term, which we thus ignore. Equations (4) and (8) then imply that the brittle-to-ductile transition crossover, $K_{Ie} = K_{Ic}$, corresponds to

$$\gamma_{us}/\mu b = 0.014. \quad (9)$$

Again, the crossover criterion is *independent* of γ_s . As in Fig. 2, the surface energy factors out of the brittle-to-ductile transition criterion. Our numerical value for the crossover criterion is only 15% higher than that from the simulations. The consistency of the analytic results with the atomistic ones suggests that our atomic simulation results have at least a rough universal validity, when allowance is made in Eq. (9) for differing factors of Y and differing atomic geometries in the calculation of Ω^s .

In conclusion, our simulations in the 2D hexagonal lattice, as well as our analytic model, have shown that for a variety of force laws, the ductile-brittle crossover is independent of γ_s , and is determined by a critical value of the γ_{us} , only. Our new finding is striking in that all previous criteria express the crossover as a competition between the values of γ_s and γ_{us} (or its equivalent dislocation core size parameter [9]). That is, a low ratio of γ_s/γ_{us} would imply a brittle material. Our criterion replaces this competition with a simple critical value for γ_{us} , and the underlying physics dictates that γ_s cancels out of the final crossover criterion. It is interesting that the new criterion for the ductile-brittle crossover is equivalent to a structure-dependent critical value for the Peierls energy of the dislocation in the material. That is, materials for which the Peierls energy of the (unfaulted)

dislocation is below a critical value are also materials which are intrinsically ductile.

We do not have the space here to enter into an extensive analysis of the general implications of this result for material intrinsic ductility, but note that one interesting fallout is that embrittlement can no longer be interpreted as due merely to a lowering of the surface energy at the crack tip, but must be a more complex phenomenon associated with changes in Ω^s as well.

We are grateful for numerous illuminating discussions regarding all aspects of the dislocation emission problem with James Rice, Glenn Beltz, and Peter Anderson. We have also benefited from comments by Mark Eberhard. This work was supported by the Office of Naval Research under Grants No. N00014-92-J-4049 at Washington University and also in part by the ONR at NIST.

*Present address: Engineering Science and Mechanics Department, Virginia Polytechnic Institute and State University, Blacksburg, Virginia 24061-0219.

- [1] J. R. Rice and R. Thomson, *Philos. Mag.* **29**, 73 (1974).
- [2] J. Weertman, *Philos. Mag. A* **43**, 1103 (1981).
- [3] G. Schoeck, *Philos. Mag. A* **63**, 111 (1991).
- [4] J. R. Rice, *J. Mech. Phys. Solids* **40**, 239 (1992); see also Y. Sun, G. E. Beltz, and J. R. Rice, *Mater. Sci. Eng.* (to be published).
- [5] R. Thomson, *Solid State Phys.* **39**, 1 (1986).
- [6] K. Cheung, S. Yip, and A. S. Argon, *J. Appl. Phys.* **69**, 2088 (1991).
- [7] G. J. Dienes and A. Paskin, *J. Phys. Chem. Solids* **48**, 1015 (1987).
- [8] R. G. Hoagland, M. S. Daw, S. M. Foiles, and M. I. Baskes, *J. Mater. Res.* **5**, 313 (1990).
- [9] S. J. Zhou, A. E. Carlsson, and R. Thomson, *Phys. Rev. B* **47**, 7710 (1993).
- [10] R. Thomson, S. J. Zhou, A. E. Carlsson, and V. K. Tewary, *Phys. Rev. B* **46**, 10613 (1992).
- [11] J. H. Rose, J. R. Smith, and J. Ferrante, *Phys. Rev. B* **28**, 1835 (1983).
- [12] J. R. Rice (private communication).

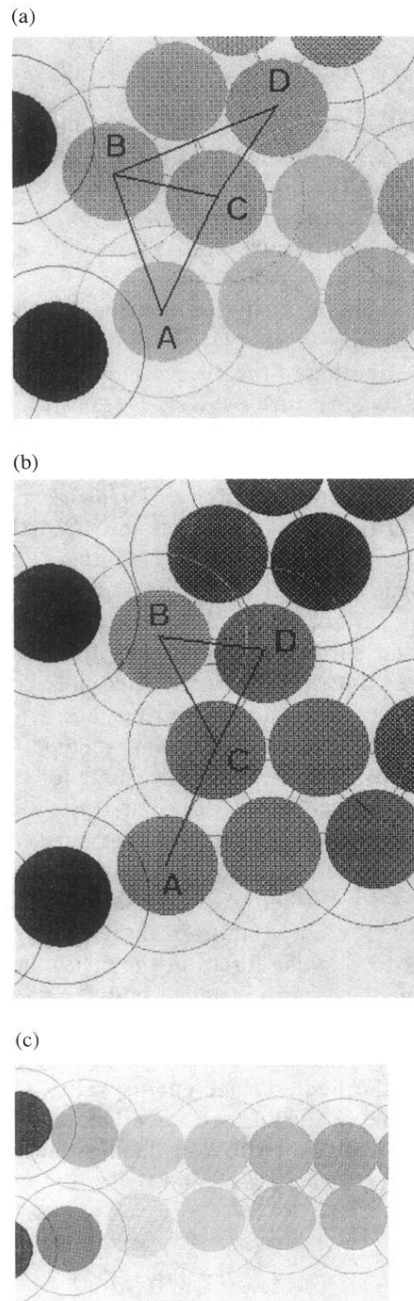


FIG. 1. Atomic positions near crack tip (a) immediately before emission in mode I; (b) immediately after emission in mode I; and (c) immediately before emission in mode II. Lighter shaded atoms are those which experience the greatest force contributions across the cohesive zone.